PRELIMINARY DESIGN AND MODELLING OF A GAS-FIRED THERMOELECTRIC GENERATOR

by

Adam KLIMANEK [a], Wojciech J. KOSTOWSKI [a*], Grzegorz BURDA [a], Pawel BARGIEL [a], Andrzej SZLEK [a], and Krzysztof GORNY [b]

[a] Institute of Thermal Technology, Silesian University of Technology, Gliwice, Poland
[b] Gascontrol Polska sp. z o.o., Suszec, Poland

The paper discusses modelling of coupled heat transfer and electricity generation in a thermoelectric generator designed for reliable island-mode power supply. The considered generator is a new concept of a low power supply (50 W) whose aim is to provide electricity for remote gas pressure reduction stations with the purpose to maintain the control and automation equipment. This equipment contributes to the system safety and minimizes the risk of unintended methane emissions. The thermoelectric generator is designed for reliable and maintenance-free operation and power supply. Natural gas is burned in a partially premixed burner and the flue gas heats the hot side of the thermoelectric generator. The combustion air cools the cold side of the thermoelectric generator, providing the temperature difference required for electricity generation occurring based on the Seebeck effect. The flow of air and flue gas through the system is driven by chimney draft. The developed model couples the heat transfer on the hot and the cold side, as well as the generation of electrical energy inside the thermoelectric modules. The model takes into account convection and conduction in the gas flow conduits and in finned heat exchangers of the cold and hot sides. The analysis demonstrates the relevance of design and operational parameters on the boundary temperatures of the thermoelectric modules. The obtained results will be used in further (ongoing) phase leading to the design and construction of a prototype electricity generator dedicated for island-mode supply.

Key words: *thermoelectric generator, heat transfer, numerical modelling, pressure letdown stations*

Introduction

Natural gas (NG) is one of the world's key energy resources, contributing to 23.7% of the global primary energy consumption in 2014 [1]. Due to large distances between the regions of extraction and consumption, there is a need of an extensive transportation infrastructure comprising high-pressure transmission pipelines, and distribution pipelines operated at several pressure levels, used to supply the gas to final consumers. The total length of distribution pipelines is by about one order of magnitude higher than that of the transmission pipelines (for example, in Poland these lengths are 160,000 km *vs.* 10,000 km).

Levels of pressure used for NG distribution depend on national regulations, in the case of Poland typical values set at the source point of each level are: 800-1,000 kPa (intermediate), 280 kPa (medium) and 2.5 kPa (low pressure). Pressure reduction (regulation) be-

---

* Corresponding author; e-mail: wojciech.kostowski@polsl.pl

tween various levels is carried out in pressure letdown stations (PLS, also called pressure reduction stations); the number of PLS in Poland is about 3,500.

Transportation of natural gas involves some losses of the transported medium. As demonstrated by Stanek and Bialecki [2], the level of leakage equal to 4.2% would offset the environmental benefits of natural gas compared to hard coal. Hence, it is essential to constantly enhance the quality of gas transmission and distribution in order to minimize possible losses.

Unfortunately, losses from distribution networks are more complex to quantify than those from the transmission pipelines. This is due to the following factors:
−   higher length of network,
−   topological complexity of the network (number of nodes),
−   limited number of gas flow metering systems,
−   limited coverage of the existing SCADA systems,
−   smaller size and impact of individual leakages, and
−   lack of information exchange platforms (such as GIE [3] and EGIG [4] for transmission pipelines).

For distribution networks, the main points of metering are the PLS, typically supplied with a gas flow meter and a volume corrector (or a flow computer). In many cases (about 1/3 of PLS in Poland), the PLS is not supplied with electric energy for economic reasons. Such *unplugged* PLS can correctly operate in the gas distribution system, and can store the measurement data in a local, battery-operated volume corrector. However, it is not possible to include the PLS into the operator's supervisory control and data acquisition (SCADA) system, which allows monitoring and controlling the gas flow and detecting possible losses.

There are two failure scenarios including natural gas emission, which remain undetectable for this class of objects:
−   medium-size network failure; the leakage flow rate does not exceed the PLS capacity; the PLS operates correctly yet the flow rate is much higher than normally; (small-size leakages remain undetectable even under SCADA supervision, large-size failures exceeding the PLS capacity entail a strong pressure drop in the network which closes the PLS slam-shut valves), and
−   failure in the PLS pressure regulators or auxiliary devices causing the safety blow-off valves to release gas to the atmosphere.

If the PLS were supplied with electrical energy and connected to the SCADA system, the operator would be able to detect the failure observing a rapid change in NG parameters (flow and pressure).

For this reason, operators of distribution networks search for island-mode supply options for the PLS objects. Available solutions comprise:
−   photovoltaic (PV) panels; this solution uses renewable energy, however, the drawback of this option is poor performance in winter period (short and poor insolation); additionally, snow fall may totally cover the panel causing downtime in power supply; the reliability of power supply is vital especially during that winter period as it is characterized by increased natural gas demand; while some PLS operate throughout the whole year, those remaining, which operate for part of the year, operate during winter season; also, the popularity of PV panels makes this option subject to thefts in remote, unsupervised locations; also, possible integration options combining PV with wind energy and diesel generator are available [5], yet these options exceed the scale of demand studied here,

− gas expanders [6]; this solution uses the exergy available in the pressurized gas; however, the available solutions are designed to produce electricity by exporting it to the public grid, and
− thermoelectric generators fired with natural gas available on-site; the solution is the subject of the research presented in this paper.

Thermoelectric generators (TEG) are based on the Seebeck effect, where two different materials whose ends are placed in sources of different temperatures, provide a different current response to the temperature gradient, creating a current loop. The Seebeck effect is usually utilized for temperature or heat flux measurements [7]. However, it is also possible to apply the effect for power generation. In energy engineering, TEG are usually considered as an option for low-grade heat recovery [8]. In the studied case, the TEG is integrated with a heat source generated intentionally, using a small share of chemical energy transported as natural gas.

Preliminary design and considerations

Estimation of the required electric output

The main objective of the designed TEG device is to provide autonomous power supply in order to include the PLS object into the operator's SCADA system (telemetry). In small PLS objects not integrated with the SCADA system, the metering line consists of:
(1) a turbine or rotary type volumetric gas meter, and
(2) a battery-supplied volume corrector with a built-in pressure sensor and an integrated RTD temperature transmitter.

The battery-supplied volume correctors convert the signals of volumetric increment (ΔV), pressure (p) and temperature (T) into short-time quantities of normalized gas volume (ΔV_n at 101.325 kPa, 0 °C), and provide an integration of these quantities over time. The volume correctors are installed directly at the metering line, within the 2nd explosion-hazard area of the metering station. The measured data and the resulting metering information are stored in the device's memory and can be accessed locally by connecting to a PC, tablet or a smartphone.

In order to integrate a PLS into the SCADA system, the metering chain should be extended to:
(1) a turbine or rotary type volumetric gas meter (no changes required if old objects are adapted),
(2) a separate pressure and temperature transducers (installed within the explosion-hazard area),
(3) a flowcomputer supplied from 230 V mains, installed beyond the explosion-hazard area, and
(4) a communication modem with a dedicated transmission interface.

The flowcomputer represents an extended version of a battery-supplied volume corrector. This class of devices is equipped with additional inputs and control outputs, enabling one to monitor multiple gas meters, and to provide digital output information for the SCADA system. The last element of the chain is a modem providing communication in one of the chosen data protocols (TCP/IP, UDP, FTP).

Power input for the described system can be evaluated based on the devices offered by the company PLUM (Bialystok, Poland [9]), applied in the majority of PLS in Poland. Accordingly, the required input is:

1236

Klimanek, A., *et al.*: Preliminary Design and Modelling of a Gas-Fired …
THERMAL SCIENCE: Year 2016, Vol. 20, No. 4, pp. 1233-1244

− 30 W for the flowcomputer type MacMAT IIIE, and
− 1.2 W for the communication modem type IK-301 3,5 G.

Due to the possible increment of input power requirements in future applications, the power output of the proposed TEG device has been assumed at the level of 50 W.

In some cases, the TEG device may be also used to provide power for an injection-type odorising equipment. Here, the range of the required power may vary depending on the type of equipment. The odorising equipment offered by Gascontrol Polska (OSGC-03) requires 50 W power input, accordingly the proposed TEG output power for this cases should yield 100 W.

Finally, it has been assumed that the prototype should be designed in two versions
(1) Basic, 50 W electric output, and
(2) Extended, 100 W electric output.

Preliminary design of the device

The TEG in design combines the functions of a combustion chamber and two heat exchangers. The hot side heat exchanger is designed to transfer heat from the hot products of combustion into the hot side of thermoelectric (TE) modules. The cold side heat exchanger should receive the heat flux from the cold side of TE modules, and reject it into a cold heat sink.

Preliminary calculations demonstrate that the cold side heat exchanger placed in the ambient air is not able to effectively dissipate the heat flux from the TE modules. This entails that the temperature difference across the TE module is very low, and the generated electric power drops to nearly zero.

Hence, it is required to increase the intensity of cooling by placing the cold-side heat exchanger into a cold agent with a sufficiently high convective heat transfer coefficient. The available solutions comprise: forced convection (fan), using a liquid or intensifying the natural convection. Using a fan is not desired since it would consume a significant part of the generated electricity, moreover, it would strongly decrease the reliability of the device which is intended to operate without constant supervision. Using a liquid complicates the construction of the device and is currently not considered. Therefore, it was proposed to intensify the convection by means of a chimney draft available in the device.

The proposed solution uses the flux of air supplied to the burner for cooling the cold-side of the generator. Following the combustion of fuel (in the designed case: natural gas) in the burner, how flue gases leaving the combustion zone flow over the hot-side of the generator. Once the flue gases are cooled in this zone, they are discharged to the environment through an exhaust channel (chimney). The chimney draft is driving the process, and causes movement of both hot flue gases and cold atmospheric air entering the device.

The flow of the cold and the hot agents at both sides of the TEG can be arranged as co-current or counter-current, which affects the temperature distribution in the heat exchanger (fig. 1). Curves in fig. 1 represent the expected (not yet calculated) distribution based on basic heat exchanger characteristics found in heat transfer handbooks [10].

As it can be seen in fig. 1, a co-current arrangement is bound to a large temperature difference at the channel head, and the difference drops towards the tail end of the channels. The advantage of this arrangement is a relatively stable temperature profile at the TE module (more exactly, at its hot and cold side). For the purpose of preliminary modelling, it is assumed that the TE modules form a continuous layer.

The counter-current flow arrangement is related to a monotonous (falling) temperature distribution across the channels and it provides a higher mean temperature difference. However, the temperature profile in the TE zone is more variable.

Possible technical arrangements of the co-current and counter-current flow are presented in fig. 2. It can be seen that the counter-current flow can be obtained using a simpler (less complex) design of the equipment. Air supplied to the devices passes below the cold side of the TE modules, and receives heat from the modules. Pre-heated air is then supplied to the burner, where combustion takes place. Hot combustion products flow over the thermoelectric modules. In order to intensify the heat transfer from the modules to the cold air, rectangular fins are placed in the inlet air channel (yellow-marked area in fig. 2).
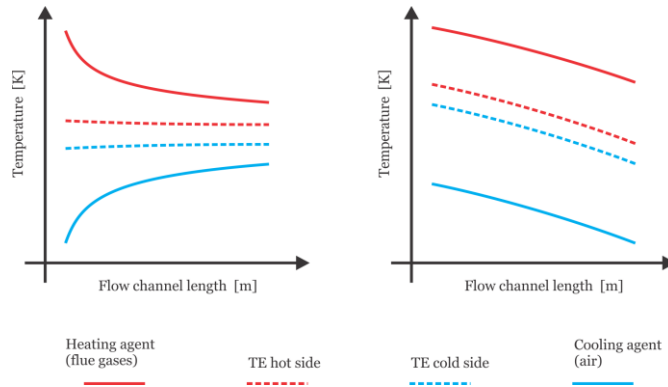

Figure 1. Expected temperature distribution in the designed device in the case of co-current (left) and counter-current (right) flow arrangements. TE modules form a continuous layer (for color image see journal web site)

Figure 2. A possible counter-current (left) and co-current (right) flow arrangement (for color image see journal web site)

In the case of the co-current flow, it is necessary to combine the zone of cold-inlet air with the zone of hot exhaust gases directly downstream of the burner. This is technically complex, since it requires using an additional (thermally idle) channel for air, since the pre-heated air is located far away from the burner.

For the present preliminary model, the counter-current flow arrangement is assumed. In fig. 3 a more detailed schematic diagram of this arrangement is presented. In the first step, only the mean temperature values across the channel length are considered, in order to determine basic factors influencing the temperature distribution across the wall (between the hot and the cold side).
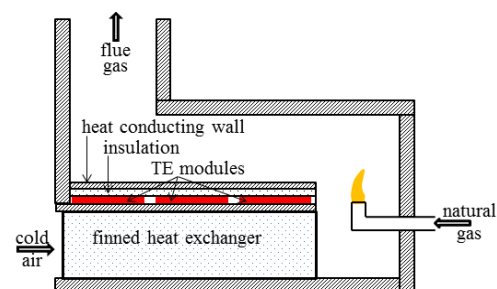

Figure 3. Schematic diagram of the considered counter-current flow arrangement (for color image see journal web site)

It should be repeated, that the heat transfer at the cold side is intensified be fins. It is expected that the fins equalize the temperature distribution along the flow channels, such that for the preliminary model, a uniform temperature distribution is assumed.

On the contrary, at the hot side of the generator, heat transfer should be limited in order to maintain the temperature at the hot side of the generator above the technological limit. For the considered type of the module, this limit equals 320 °C. In order to protect the module from excessive temperature, thermal insulation is installed between the hot exhaust gas and the thermoelectric modules.

Model equations

Heat transfer from the hot to the cold side of the generator comprises:
- convection from the flue gas to the hot side walls of the device,
- conduction through an insulation layer,
- heat transfer through a thermoelectric module with generation of electricity, and
- convection from the finned cold side walls to the cooling air.

Heat transfer at the hot side eq. (1) of the generator is calculated from the convection heat transfer coefficient directly integrated over the wall surface:

$$\dot{Q}_1 = A_1 h_1 (T_1 - T_{w1}) \tag{1}$$

Heat transfer at the cold side eq. (2) of the device equals the heat transfer rate at the hot side reduced by the generated flux of electric energy:

$$\dot{Q}_2 = \dot{Q}_1 - N \tag{2}$$

On the other hand, the heat transfer rate at the cold side results from the local heat transfer conditions. For a finned surface, the total rate is composed of the heat transfer from the fins and from the space between them [10]:

$$\dot{Q}_2 = n A_{2F} k_2 (T_{w2} - T_2) m \tanh(mL) + A_{2B} h_2 (T_{w2} - T_2) \tag{3}$$

where n is the number of fins, A_{2F} is the cross section area of a single fin, k_2 is the fin's material thermal conductivity, L is the fin's height (from the base), A_{2B} is the wall surface between the fins, and m is the fin parameter defined as:

$$m = \sqrt{\frac{2h_2}{k_2 y}} \tag{4}$$

where y is the thickness of the fin.

The convection heat transfer coefficients h_1 and h_2 have been determined from the following empirical formulae [10]:

$$\text{Nu} = \begin{cases} 0.74\, \text{Pe}^{0.2} (\text{GrPr})^{0.1} \varepsilon_t \varepsilon_1 & \text{if } \text{Re} < 2{,}300 \\ 0.021\, \text{Re}^{0.8} \text{Pr}^{0.43} \varepsilon_t & \text{if } \text{Re} \geq 2{,}300 \end{cases} \tag{5}$$

where ε_1 is a correction factor for the channel starting section, and ε_t is a factor accounting for the difference between the fluid properties for the wall w and the mean boundary layer temperature f:

$$\varepsilon_t = \left(\mathrm{Pr}_f / \mathrm{Pr}_w\right)^{0.25} \tag{6}$$

Due to the limitations of the hot side temperature of TE modules, a thermal insulation has been applied to protect the modules against excessive temperature. Provided that the heat flux density at the hot side is given by eq. (1), it can be written:

$$\dot{q}_1 = \frac{\dot{Q}_1}{A_1} \tag{7}$$

and the temperature at the hot side of the TE modules can be found from the condition:

$$T_{TE1} = T_{w1} - \dot{q}_1\left(R_{w1} + R_i\right) \tag{8}$$

where R_{w1} and R_i are the thermal resistances of the channel wall and the insulation, calculated as the quotient of the corresponding thickness and conductivity:

$$R_i = \frac{\delta_i}{k_i} \tag{9}$$

Heat transfer calculations for the layer including the thermoelectric modules is based on the following assumptions:
– TE modules cover the entire space between the insulation and the outer (cold-side) wall of the device,
– electrical energy generated in the modules is small compared with the heat transfer rate; this means that the results of the heat transfer model determine the electric power, but the electric power has a negligible impact on the heat transfer model; this assumption is done for the first iteration, and is then corrected in subsequent iterations, as described in section *Solution algorithm*, and
– there are no heat losses in the heat transfer through the TE modules.

Knowing the thermal conductivity of the TE module and the corresponding thermal resistance R_{TE} it is possible to obtain the cold side temperature:

$$T_{TE2} = T_{TE1} - \dot{q}_1 R_{TE} \tag{10}$$

Once the cold-side temperature T_{TE2} is known, it is possible to obtain the power generated by the modules. The estimation of TE power output is done based on characteristic curves provided by the manufacturer [11] and approximated by the following functions:

$$N = \begin{cases} a_0 + \left[a_1 + a_2\left(\vartheta_{TE2} - a_4\right)\right]\Delta T + a_3\left(\vartheta_{TE2} - a_4\right) & \text{if } \vartheta_{TE1} > 250\,°\mathrm{C} \\ b_1\Delta T + b_2\left(\Delta T\right)^2 + b_3\left(\Delta T\right)^3 + b_4\left(\Delta T\right)^4 & \text{otherwise} \end{cases} \tag{11a-b}$$

where ϑ has to be given in °C, and ΔT is the temperature difference across the TE module ($\Delta T = T_{TE1} - T_{TE2}$). Original characteristic curves are presented in fig. 4, and the values of the approximation function coefficients are given in tab. 1.

It should be underlined that the manufacturer indicates the TE output for T_{TE1} in the range (50 °C-300 °C) and T_{TE2} in the range (25 °C-100 °C). In order to make the model continuous outside this range the data is extrapolated. If the temperature of the hot side of the generator T_{TE1} exceeds the value of 100 °C, the extrapolation is done by eq. (11a). If the temperature of the cold side of the generator exceeds 100 °C, extrapolation is done by the following linear interpolation:

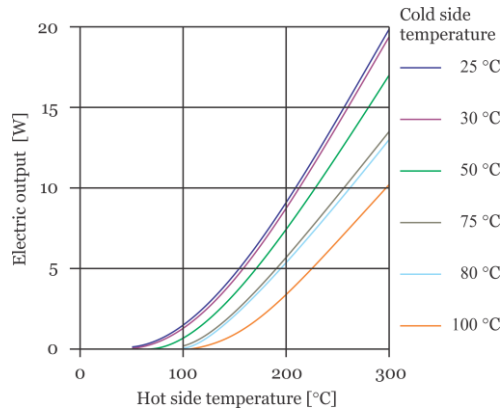**Figure 4. Electric output of the analysed TE module in terms of its boundary temperatures** (for color image see journal web site)

$$N = N\left(\vartheta_{TE1}, 100\ °C\right)\left(1 - \frac{\vartheta_{TE2} - 100}{\vartheta_{1TE} - 100}\right) \quad (11c)$$

which yields 0 if both temperatures are equal.

Finally, the efficiency of the generation is calculated by comparing the power output with the heat transfer rate supplied to the hot side of the device:

$$\eta_{TE} = \frac{N}{A_{TE}\ \dot{q}_1} \quad (12)$$

Solution algorithm

Heat transfer and energy balance equations have been set in a series of functions written in MATLAB environment [12] which is coupled with a chemistry simulation tool Cantera [13]. Each module contains equations for one part of the device, as shown in fig. 5.

At the current stage of development of the model, the flow rates of air and gas are fixed in such a way that for a given mass flow rate of fuel and for a given air-fuel equivalence ratio, the air flow rate at the inlet to the cold side heat exchanger is determined. When the solution is

Table 1. Coefficients of the approximation functions for TE electric output

Coefficient	Value	Coefficient	Value
a0	−5.853	b1	−3.489E–3
a1	8.706E–2	b2	4.780E–4
a2	−3.827E–4	b3	−1.190E–6
a3	5.600E–2	b4	1.924E–9
a4	62.51		

initialized, particular temperatures are not known. First of all, energy balances of the combustion chamber are resolved, with the assumption that the air temperature at the combustion chamber inlet is equal to the ambient air temperature. This allows to determine the composition and temperature of the outlet gas. It is assumed that the combustion is complete, *i. e.* the combustion products are only composed of CO_2, H_2O, N_2 and O_2. Then, the hot gas temperature is used to initialize the mean wall temperature of the hot side heat exchanger. With these data the heat flux from flue gases, through the hot side heat exchanger, insulation, thermoelectric modules and the cold side heat exchanger to the air is determined according to eqs. (1)-(10). This allows calculating both the power generated by the TGE, as well as the enthalpy increase of air entering the cold side heat exchanger. The air temperature at the inlet to the combustion chamber is then updated to a new value. This starts another loop of the calculations as described above. The computations are repeated until the energy in the system is balanced, *i. e.* the heat transferred from the hot side to the cold side, with the heat flux drop at the TEG, does not change the air temperature at the combustion chamber inlet anymore.

Model elements, which are external to the main loop are the model geometry set by a series of design parameters (channel width, height, dimensions of the fins, distance between the fins, thickness of insulation), the properties of solid materials (thermal conductivity) and the properties of gases (thermal conductivity, kinematic viscosity, specific heat). Density of gas is determined from ideal-gas equation of state. Another parameters external to the main loop are the natural gas stream and the air/fuel equivalence ratio, which may be varied in order to achieve the desired exhaust gas temperature supplied to the hot side of the device.

Particular care has been taken to accurately represent the properties of gases (air and flue gas) which are required at many stages of the computations. The properties are calculated by means of the Cantera software.
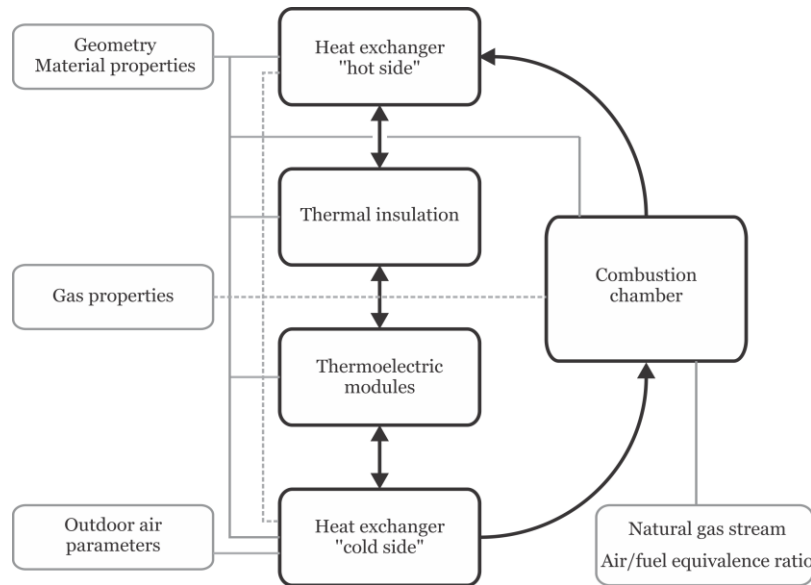

Figure 5. Outlay of the solution algorithm for heat transfer and energy balance

The function *thermoelectric modules* contains the characteristic curves of the modules and additional logical conditions which issue several types of warnings (flags) if:
− one or both temperatures are out of the allowed range,
− one or both temperatures are beyond the design range, in this case the power output is extrapolated and can not be guarranted, and
− the cold-side temperature is above the hot-side temperature (if so, power is set to zero).

Results and discussion

Since the objective of operation of the TEG in-design is to provide electric output, it is essential to find the boundary temperatures at the hot and the cold side of the thermoelectric modules, which are hidden inside the device.

Figure 6 presents the distribution of mean temperature across the device. On the left side of the figure (distance = 0.0 m), the mean temperature of gases at the hot side is marked, while the right side (distance = 0.32 m) represents the mean temperature of inlet air at the cold side. The most significant values, *i. e.* the boundary temperatures of the TE modules can be seen in the central part of the graph. The temperature distribution has been presented for various air-fuel equivalence ratio.

It can be seen that the air-fuel ratio strongly influences the temperature level in the device. Lower ratios correspond to higher temperatures and are potentially more interesting due to a higher temperature gradient across the module (which can be seen as the inclination of the temperature curve between the two central points in the graph). Unfortunately, material limitations require the temperatures at the TEG to be maintained below specified limits (for

the studied case, 320 °C at the hot side and 180 °C at the cold side). Accordingly, higher air-fuel ratios are needed to 'dilute' the exhaust gases.

Moreover, it is important to observe the impact of inlet air temperature which varies strongly under the climatic conditions of Poland. Figure 7 presents both boundary temperatures of the TE module (hot and cold side) in terms of the air-fuel equivalence ratio and in terms of the inlet air temperature. It can be seen that the 'climatic sensitivity' of the device is significant, although the changes in the TE boundary temperatures are slightly weaker than the changes in the inlet air temperature. The assumed variation of the ambient air temperature is 60 K, the corresponding obtained variation at the TE hot side ranges between 51 and 56 K, and on the TE cold side: between 51 and 57 K.
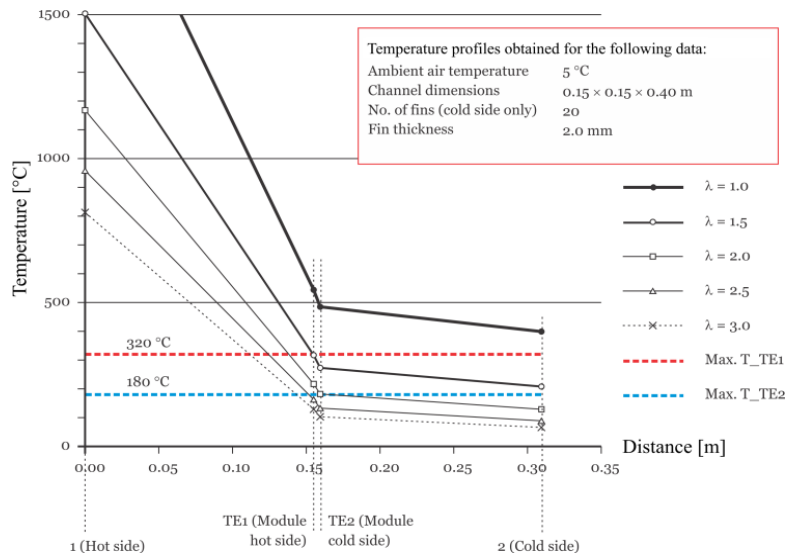

Figure 6. Temperature profile across the walls of the device in terms of the air-fuel equivalence ratio (λ) (for color image see journal web site)

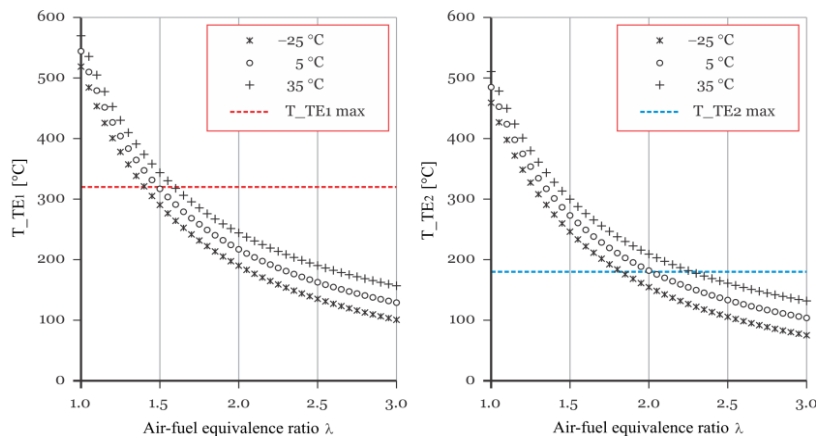**Figure 7. Temperature at the hot (left) and cold (right) side of the thermoelectric modules in terms of the air-fuel equivalence ratio** (λ) (for color image see journal web site)

Also, as shown in tab. 2, a higher number of fins provides a more favorable temperature distribution across the device, since the temperature gradient across the TE module slightly increases, and the temperature level in the TE zone decreases.

However, it can be seen that for all studied parameters, the temperature drop across the module is below 50 K which corresponds to low power output according to the manufacturer's data. It can be supposed that higher temperature drops, claimed by the manufacturer, were obtained only during a limited period of time, until the cold side of the module reached

Table 2. Temperature profile: sensitivity to the number fins (*n*) at the cold side. Data obtained for the air-fuel equivalence ratio of 2.0

Point	Temperature [°C]		Change [K]
	n = 20 (reference)	*n* = 40	
1. Hot side (flue gas)	1,168.2	1,170.6	+2.4
TE1: TE hot side	217.1	198.8	−18.3
TE2: TE hot side	181.9	162.8	−19.0
2. Cold side (air)	129.3	132.2	+3.0

its target temperature due to heat conduction across the thin semiconductor layer.

Conclusions

According to background information collected prior to the realization of the project, the main problem in the design of thermoelectricity generators is the effective cooling at the cold side of the modules. This fact has been confirmed by the preliminary model presented herewith.

Due to the insufficient heat transfer rate at the TEG cold side, the temperature drop across the module (and accordingly, the generated power output) is lower than desired from the point of view of TEG characteristic curve. It may be concluded that natural convection sets a remarkable limitation here. However, an optimization procedure comprising both the operating principle and design parameters (in particular, dimensions) can significantly improve the performance of the device.

Another problem observed is the excessive temperature level in the TEG zone. In order to maintain the TEG boundary temperatures (especially, the hot side temperature) within material-related limitations, it is required to reduce the source temperature, which is possible either by applying thermal insulation between the hot exhaust gases and the TE zone, or by reducing the temperature of hot gases by increasing the air-fuel equivalence ratio. Both options are related to exergy losses, and the latter option directly entails a loss of energy efficiency similarly like for the gas turbines. Higher allowable temperatures can be achieved if very expensive materials are used for the TEG.

The preliminary study presented here provides a first view on the system's performance and illustrates difficulties which have to be addressed in the design process. Further work, leading to an optimum design of the device is currently continued by means of CFD modelling along with a series of experimental tests, and the results will be presented in the nearest future.

Acknowledgment

Nomenclature

A – surface area, [m^2]
a – thermal diffusivity, [m^2s^{-1}]
Gr – Grashof number ($= g\beta\Delta TL^3/v^2$), [–]
g – gravitational acceleration, [ms^{-2}]
h – convection heat transfer coefficient, [$Wm^{-2}K^{-1}$]
k – thermal conductivity, [$Wm^{-1}K^{-1}$]
L – characteristic length, [m]
m – fin performance parameter, [m^{-1}]
N – electric power, [W]
Nu – Nusselt number ($= hL/k$), [–]
Pe – Péclet number ($= uL/a$), [–]
Pr – Prandtl number ($= v/a$), [–]
$\dot{Q}$ – heat transfer rate, [W]
$\tilde{q}$ – heat flux, [Wm^{-2}]
R – thermal resistance, [m^2KW^{-1}]
Re – Reynold number ($= uL/v$), [–]
T – temperature, [K]
ΔT – wall-bulk fluid temperature difference, [K]

u – flow velocity, [ms^{-1}]
y – fin thickness, [m]

Greek symbols

β – thermal expansion coefficient, [K^{-1}]
δ – layer thickness, [m]
ε_l – correction factor: starting section
ε_t – correction factor: boundary layer
η – efficiency
ϑ – temperature, [°C]
λ – air-fuel equivalence ratio
v – kinematic viscosity, [m^2s^{-1}]

Subscripts

f – mean parameters of the boundary layer
TE – thermoelectric module
w – wall
1 – hot side
2 – cold side

References

[1] ***, BP Statistical Review of World Energy 2014, http://www.bp.com/statisticalreview
[2] Stanek, W., Bialecki, R., Can Natural Gas Warm the Climate More than Coal?, *Fuel*, *136* (2014), Nov., pp. 341-348
[3] ***, Gas Infrastructure Europe, Information Exchange Platform, http://www.gie.eu
[4] ***, European Gas Pipeline Incident Data Group, http://www.egig.eu
[5] Katti, P. K., Khedkar, M. K., Alternative Energy Facilities Based on Site Matching and Generation Unit Sizing for Remote Area Power Supply, *Renewable Energy*, *32* (2007), 8, pp. 1346-1362
[6] Kostowski, W., The Possibility of Energy Generation Within the Conventional Natural Gas Transport System, *Strojarstvo*, *52* (2010), 4, pp. 429-440
[7] Sippawit, N., Leephakpreeda, T., A Study of Sensing Heat Flow through Thermal Walls by Using Thermoelectric Module, *Thermal Science*, *19* (2014), 5, pp. 1497-1505
[8] Xiao, H., *et al.*, Detailed Modeling and Irreversible Transfer Process Analysis of a Multi-element Thermoelectric Generator System, *Journal of Electronic Materials*, *40* (2011), 5, pp. 1195-1201
[9] ***, Manufacturer's Website, http://www.plum.pl
[10] Kostowski, E., *Heat transfer*, Silesian University of Technology Publishing House (in Polish), Gliwice, Poland, 2006
[11] ***, Manufacturer's Website, http://www.customthermoelectric.com
[12] ***, MATLAB, version 7.9.0.529 (R2009b), The MathWorks Inc., Natick, Massachusetts, 2009
[13] ***, Cantera, Software provider's website, http://www.cantera.org